

December 28, 2011

U. S. Nuclear Regulatory Commission
ATTN: Document Control Desk
Washington, DC 20555-0001

**Subject: Docket Nos. 50-361 and 50-362
Response to Request for Additional Information Regarding Use of
American Concrete Institute (ACI) Reports for Restoration of Unit 3
Containment (TAC Nos. ME6179 and ME6180)
San Onofre Nuclear Generating Station, Units 2 and 3**

Reference: Letter from J. R. Hall (NRC) to P. T. Dietrich (SCE) dated October 14,
2011; Subject: San Onofre Nuclear Generating Station, Units 2 and 3 -
Request for Additional Information Regarding Use of American Concrete
Institute (ACI) Reports for Restoration of Unit 3 Containment (TAC Nos.
ME6179 and ME6180)

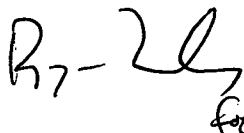
Dear Sir or Madam:

By letter dated October 14, 2011, the Nuclear Regulatory Commission (NRC) issued a Request for Additional Information (RAI) (Reference) regarding use of American Concrete Institute (ACI) Reports for restoration of Unit 3 containment. The enclosure provides Southern California Edison's (SCE's) response.

The RAI letter requested a response within 30 days of receipt of the letter. NRC staff agreed by phone on December 14, 2011, that SCE may submit the response by December 30, 2011.

There are no new regulatory commitments contained in this letter. If you have any questions or require additional information, please contact Ms. Linda T. Conklin at (949) 368-9443.

Sincerely,


R.S.O.

Enclosure: Response to Request for Additional Information Regarding Use of American Concrete Institute (ACI) Reports for Restoration of Unit 3 Containment

cc: E. E. Collins, Regional Administrator, NRC Region IV
R. Hall, NRC Project Manager, San Onofre Units 2 and 3
G. G. Warnick, NRC Senior Resident Inspector, San Onofre Units 2 and 3

Response to Request for Additional Information Regarding Use of American Concrete Institute (ACI) Reports for Restoration of Unit 3 Containment

RAI 1

In Section 5.1 of Calculation C-257-01.04.05 (Reference 1), the licensee stated:

The new concrete mix for restoration of the containment opening will be tested to determine the compressive strength, the modulus of elasticity and the creep characteristics. However, the results will not be available at the time for the EOL [end of life] finite element analysis. As such, the methods described in ACI 209R-92 and ACI 318-05 are used to estimate the relevant concrete properties. The moduli of existing and new concrete as well as creep and shrinkage will be used in the containment analysis to investigate the stress distribution around the opening after restoration.

The licensee's position on the use of ACI 209R-92 is further summarized as follows:

The ACI 209R Report is a widely recognized guidance document that provides a simple, yet reasonably accurate methodology for estimating creep and shrinkage design values. For the SONGS containment structure, the use of such estimated values has been further justified and validated by comparison to long term creep and shrinkage test results performed on the actual concrete mix used to restore the temporary construction opening.

Please provide the above stated comparison of the concrete properties (creep, shrinkage, elastic modulus) obtained from tests of the actual concrete mix used for the restoration of the steam generator replacement construction opening to those used in the analysis based on estimates using methods in ACI 209R-92, "Prediction of Creep, Shrinkage, and Temperature Effects in Concrete Structures," that would demonstrate that the properties used in the SONGS containment analysis are comparable or conservative relative to those obtained from the tests. In establishing values of creep and shrinkage, please indicate how any important differences in the environment between the test samples and the actual concrete in the structure, if any, were considered.

Response to RAI 1

The creep and shrinkage study report (Ref. 8) for the new concrete, prepared by the CTL Group of Chicago, provides tested data that were developed for loading at both 7 and 28 days. The dates of the concrete pours and the dates when the vertical and hoop tendons were tensioned are provided for Units 2 and 3 in Attachment 1 to this RAI response.

Creep:

In Ref. 1, estimates of creep were made assuming loading 7 days after the concrete placement. Attachment 1 to this RAI shows that the average number of days was actually 14 days for Unit 2 and 9 days for Unit 3. Considering this, the comparison of creep coefficients obtained from tests of the actual concrete mix to that used in the analysis can be established as follows:

<p><u>Creep coefficient from tests</u></p> <p>One year with loading at 7 days $(v_{1yr})_7 = 1.235 \times 10^{-6}$ (Ref. 8)</p> <p>One year with loading at 28 days $(v_{1yr})_{28} = 0.93 \times 10^{-6}$ (Ref. 8)</p> <p>One year with loading at 9 days $(v_{1yr})_9 = 1.180 \times 10^{-6}$</p> <p>End-of-life with loading at 9 days $v_{EOL} = 1.52 \times 10^{-6}$</p> <p><u>Creep coefficient in Ref. 1</u> $v_{EOL} = 1.20 \times 10^{-6}$</p>
--

The increase in the creep coefficient will increase the creep strains by the ratio $1.52/1.2 = 1.27$. The corresponding increase in the creep losses given in Section 8.3.2.3 of Ref. 1 will be about 0.1 ksi, which is negligible compared with the average tendon stresses of about 170 ksi, per Tables 16 and 17 of Ref. 1.

Shrinkage:

The shrinkage loss that takes place prior to placement of the load on the concrete is irrelevant to prestress losses. Since the loading was applied in about 9 days after concrete placement (Unit 3), the comparison between the shrinkage strain from tests and that used in the analysis can be summarized as follows:

<p><u>Shrinkage strain from tests</u></p> <p>Ultimate shrinkage strain for a specimen loaded at 7 days: $(\epsilon_{sh})_u = 288 \times 10^{-6}$ in/in (Ref. 8)</p> <p>Shrinkage after 2 days for specimen loaded at 7 days: $(\epsilon_{sh})_7 = 72 \times 10^{-6}$ in/in (Ref. 8)</p> <p>Ultimate shrinkage for a member loaded at about 9 days: $(\epsilon_{sh})_u = 216 \times 10^{-6}$ in/in</p> <p><u>Shrinkage strain in Ref. 1</u> $(\epsilon_{sh})_u = 117 \times 10^{-6}$ in/in</p>

This is an increase of about 85% over the value used in Ref. 1. The prestress losses due to shrinkage were less than 1 ksi (Tables 16 and 17 of Ref. 1). The net increase in the prestress losses due to increase in shrinkage will be less than 0.25 ksi. Therefore, the actual prestressing loss due to shrinkage as determined by the tests has negligible impact on the design.

Elastic modulus:

The concrete modulus of elasticity at 28 days can be calculated as follows:

$$(E_c)_{28} = \sigma_s / \epsilon_c = (2100 \text{ psi}) / (463 \times 10^{-6} - 2 \times 10^{-6}) = 4555 \text{ ksi (from Ref. 8)}$$

This is an increase of about 3% over the value used in Ref. 1, which has negligible effect on analysis results.

The creep and shrinkage test report for the original containment construction (Ref. 3) indicates that a seal was provided to the concrete cylinders as shown below:

2.0 TEST PROGRAM (Excerpt from Ref. 3)

The test program comprises the evaluation of the following properties on two concrete mixes, one with 3/4 in., and other with 1 1/2-in. maximum size aggregate. Both of these mixes are designated for $f_c = 6000 \text{ psi @ 90 days}$.

- 2.1 Compressive strength to be determined on three 6-in. by 12-in. sealed concrete specimens, stored at 73°F. at ages of 7, 28, 90, 180 and 365 days.
- 2.2 Modulus of Elasticity and Poisson's Ratio to be determined on three 6-in. by 12-in. sealed concrete specimens, stored at 73°F, at ages of 28, 180 and 365 days.
- 2.3 Coefficient of Thermal Expansion to be determined on two 6-in. by 16-in. sealed concrete specimens, stored at 73°F, at ages of 28, 90, 180 and 365 days.
- 2.4 Diffusivity to be determined on two (total of four) 8-1/2-in. by 17-in. sealed concrete specimens, stored at 73°F, at age of 90 days.
- 2.5 Creep Characteristics of sealed concrete specimens to be determined at a sustained stress of 2100 psi initially applied at ages of 28, 180, and 365 days. The autogenous strains changes for specimens stressed at ages of 28 and 180 days shall be determined from sealed creep specimen that will be stressed at age one year. Changes in autogenous strains are small after the age of one year; therefore, no corrections of autogenous strains will be applied to creep specimens stressed at one year. The creep tests shall be carried out at 73°F. Each creep test shall be conducted on a set of two 6-in. by 16-in. sealed concrete specimens.

The CTL report (Ref. 8) for creep and shrinkage tests applicable to concrete in the restored containment opening follows similar requirements for sealing concrete cylinder specimens from ASTM C 512 (Ref. 4) to prevent loss of moisture throughout the period of storage and testing.

As the thickness of the containment wall is large and the existence of the liner completely prevents any moisture loss from the inside face, the restored concrete in the structure will have insignificant moisture loss. Therefore, the environmental difference between the test samples and the actual concrete in the structure is minimal.

RAI 2

Please justify why it is acceptable to apply the methodology in Section 4-1 of the ACI 224.2R-92 report, concerning the axial stiffness of one-dimensional members due to cracking in reinforced concrete caused by direct tension, to account for cracking in: (a) prestressed concrete, and (b) more complex systems such as post-tensioned containments, for the end-of-life evaluation of the restored SONGS containments in Calculation No. C-257-01.04.06 (Reference 2).

Response to RAI 2

The methodology in Section 4-1 of the ACI 224.2R-92 report, concerning the axial stiffness of one-dimensional members due to cracking in reinforced concrete caused by direct tension, is acceptable to account for cracking in prestressed concrete provided that prestress forces and tendons are properly considered in the design of members. In other words, a prestressed concrete member can be treated as a reinforced concrete member if prestress forces are modeled as another load. (See Section 4 of Ref. 13 for general discussion on the subject.) Accordingly, in Calculation No. C-257-01.04.06 (Ref. 2) the prestress forces were considered as an external force, F , and the existence of tendons was included by accounting their tributary area in the calculation of the stiffness of a cracked member, as further shown in Response to RAI 3.

Using the ACI 224.2R-92 methodology to account for cracking in complex systems, such as post-tensioned containments, is justified by the observed behavior of containments during pressurization, which is the governing condition in this analysis. During pressurization, such as the integrated leak rate testing performed at SONGS after restoration of containment (Ref. 9 through Ref. 12), portions of containment structures subject to cracking typically develop hairline cracks that are primarily oriented in the hoop and vertical directions. This behavior confirms the one-directional response of the structure.

The complexity of the structure (including removal of a number of tendons, cutting an opening while under partial prestress, repairing the opening, post-tensioning the replaced tendons, etc.) indicates that a more complex analytical model may provide improved results for the end-of-life evaluation. However, such a complex approach was not deemed necessary to obtain a solution to the problem since (a) reasonable assumptions were made in modeling and application of loads, (b) conservative approximations were applied to maximize the critical design forces, and (c) checks were made at intermediate steps to validate the approach.

Also note that the original design calculation of the SONGS containment employed the same one-dimensional modeling methods. Where preliminary analysis indicates potential for cracking, the Updated Final Safety Analysis Report (UFSAR) method of evaluation for containment analysis, which is contained in UFSAR Subsection 3.8.1.4 (Ref. 14) and further detailed in Bechtel Topical Report BC-TOP-5, Rev. 1 (Ref. 5), requires the potential for load redistribution due to concrete cracking to be considered by adjusting the analytical model. Specifically, the method of evaluation of reducing the concrete modulus of elasticity in areas subject to cracking is consistent with the original calculations. The resulting forces are then combined in accordance with the UFSAR load combinations, and the design is carried out using one-dimensional elements in the hoop and vertical directions. This is the approved method for the original SONGS 2 & 3 containment analysis and design.

In summary, the repair design incorporating the methodology of ACI 224.2R-92 is appropriate, consistent with the approved method of evaluation for SONGS 2 & 3, and was independently reviewed by industry consultants experienced in containment analyses and similar SGR projects. All the results were

subjected to reasonableness, completeness, adequacy and appropriateness tests that are an integral part of the nuclear safety-related structural design practice.

RAI 3

Appendix H of Calculation No. C-257-01.04.06 (Reference 2) describes the methodology and criteria used, based on Equations 4.12 and 4.13 of the ACI 224.2R-92 report, to estimate a reduced concrete sectional stiffness to account for cracking in the restored containment opening area, in the ANSYS shell-element-based linear elastic finite element model of the SONGS containments.

With regard to the application of Equations 4.12 and 4.13 of ACI 224.2R to calculate the effective cross-sectional area, A_e , of a cracked member in the above calculation, please provide the following information:

- (a) For both the hoop and vertical directions, was the cross-sectional area of prestressing tendon steel included in the calculation of A_g , A_s and A_{cr} ? If not, please provide a supporting justification.

Response to RAI 3(a)

Yes, the cross-sectional area of tendons was included in the calculation of A_g , A_s and A_{cr} .

- (b) For both hoop and vertical directions, was the gross cross-sectional area, A_g , replaced with the transformed area, $A_t = A_g + (n-1)A_s$, to include the contribution of bonded reinforcing steel and unbonded prestressing steel in the post-tensioned containment? If not, please provide a supporting justification.

Response to RAI 3(b)

Yes, the gross cross-sectional area, A_g , was replaced with the transformed area, $A_t = A_g + (n-1)A_s$, to include the contribution of both bonded reinforcing steel and unbonded prestressing steel in the post-tensioned containment.

- (c) How was the cracking load, P_{cr} , calculated for the hoop and vertical directions? Please identify what values of P_{cr} were used for the hoop and vertical directions. Please indicate the material property threshold (such as tensile strength) that was used to determine the cracking load.

Response to RAI 3(c)

P_{cr} is calculated for the hoop and vertical directions using Equation (2.1) of ACI 224.2R (Ref. 7), which is shown below:

$$P_{cr} = (1 - \rho + n\rho)A_g f_t'$$

in which ρ is the reinforcing ratio, A_s/A_g ; A_s is the area of reinforcing steel plus tendons; A_g is the gross cross-sectional area; and n is the ratio of modulus of elasticity of the steel to that of concrete. The direct tensile concrete strength, f_t' , is used in this expression, which can be calculated as $4\sqrt{f_c'}$ ($\approx 0.33\sqrt{(150f_c')}$) (per Equation (3.2) of ACI 224.2R).

The calculation details and material properties that were used to determine the cracking load, P_{cr} , in each direction are shown below:

<u>Vertical direction</u>	<u>Hoop direction</u>
$A_s = 5.22\text{in}^2/\text{ft} + 3.12\text{in}^2/\text{ft} = 8.34\text{in}^2/\text{ft}$ (see Attachment C.2 and Appendix I of Ref. 2)	$A_s = 4.80\text{in}^2/\text{ft} + 5.42\text{in}^2/\text{ft} = 10.22\text{in}^2/\text{ft}$ (see Attachment C.2 and Appendix I of Ref. 2)
$A_g = 624\text{in}^2/\text{ft}$	$A_g = 624\text{in}^2/\text{ft}$
$\rho = 0.0134$	$\rho = 0.0164$
$n = 6.57$	$n = 6.57$
$f_t' = 4\sqrt{f_c'} = 310 \text{ psi}$	$f_t' = 4\sqrt{f_c'} = 310 \text{ psi}$
$P_{cr} = 208\text{kip}/\text{ft}$	$P_{cr} = 211\text{kip}/\text{ft}$

Note that the comparison with the cracking load without including reinforcing steel and tendons, that is $P_{cr} = A_g f_t' = 193\text{kip}/\text{ft}$, with values presented in the table above suggests that the contribution of reinforcing steel and tendons to the cracking load is small because the strain level at the cracking load is also small.

- (d) Please provide a numerical example of all steps (with all inputs used) of a typical calculation (e.g., for the ratio, $(E_c A_e)_{ANSYS}/E_c A_g = 0.4$ or 0.6) that was performed to develop a data point (one in hoop direction and one in vertical direction) in Figure H.2 of Reference 2.

Response to RAI 3(d)

The data point in Figure H.2 of Ref. 2 is obtained using the following procedure:

- (1) Perform ANSYS analysis with an assumed effective stiffness, E_c .
- (2) Measure the axial strain for the selected load combination along the desired direction, ϵ_{ANSYS} .
- (3) Find the effective stiffness corresponding to the axial strain obtained from ANSYS, $E_c A_e$.

The numerical example for $(E_c A_e)_{ANSYS}/E_c A_g = 0.4$ is shown below:

1. Vertical direction

ANSYS vertical strain, $\epsilon_{v,ansys}$, of (D+F+1.5P) at restored area: $E_e = 0.4E_c$

$$E_c := 57 \cdot \sqrt{\frac{6000 \text{ psi}}{\text{psi}}} \cdot \text{ksi} = 4415 \cdot \text{ksi}$$

$$E_{c,ansys} := 0.4 \cdot E_c$$

$$\epsilon_{v,ansys} := 0.00022$$

Vertical tensile strains corresponding to $E_e = 0.4E_c$ from ANSYS

Calculation of cracking load

$$A_g := 624 \frac{\text{in}^2}{\text{ft}}$$

$$A_s := 8.34 \frac{\text{in}^2}{\text{ft}}$$

$$\rho := \frac{A_s}{A_g} = 0.0134$$

$$E_s := 29000 \text{ ksi}$$

$$n := \frac{E_s}{E_c} = 6.568$$

$$f_t := 4 \cdot \sqrt{\frac{6000 \text{ psi}}{\text{psi}}} \cdot \text{psi} = 310 \cdot \text{psi}$$

Eq (3.2) of ACI 224 for $w_c = 150 \text{ lb/ft}^3$

$$P_{cr} := (1 - \rho + n \cdot \rho) \cdot A_g \cdot f_t = 208 \cdot \frac{\text{kip}}{\text{ft}}$$

Eq (2.1) of ACI 224

Uncracked section stiffness

$$EA_{un} := E_c \cdot A_g = 2755085 \frac{\text{kip}}{\text{ft}}$$

Tensile strain at cracking

$$\epsilon_{cr} := \frac{P_{cr}}{EA_{un}} = 0.000075$$

ACI 224 Calculations to find EA_e corresponding to the concrete strain of $\epsilon_{v,ansys}$

Assume an axial load $P := 250 \frac{\text{kip}}{\text{ft}} > P_{cr} = 208 \frac{\text{kip}}{\text{ft}}$ Cracked section

$A_{cr} := n \cdot A_s$ Definition given in ACI 224

$$A_e := A_g \cdot \left(\frac{P_{cr}}{P} \right)^3 + A_{cr} \cdot \left[1 - \left(\frac{P_{cr}}{P} \right)^3 \right] = 381 \cdot \frac{\text{in}^2}{\text{ft}} \quad \text{Eq (4.13) of ACI 224}$$

$$EA_e := E_c \cdot A_e = 1683630 \cdot \frac{\text{kip}}{\text{ft}}$$

$$\frac{EA_e}{EA_{un}} = 0.611 \quad E_{cr} := \frac{EA_e}{EA_{un}} \cdot E_c$$

$$\epsilon_v := \frac{P}{EA_e} = 0.00015 \quad \text{Eq (4.12) of ACI 224}$$

Therefore, the effective stiffness of $0.611E_cA$ can be related to the concrete strain of $\epsilon_v = 0.00015$.

By repeating the calculation for different axial loads, P , the relationship between the concrete strain and the corresponding effective stiffness can be obtained. The following figure shows the resulting relationship.

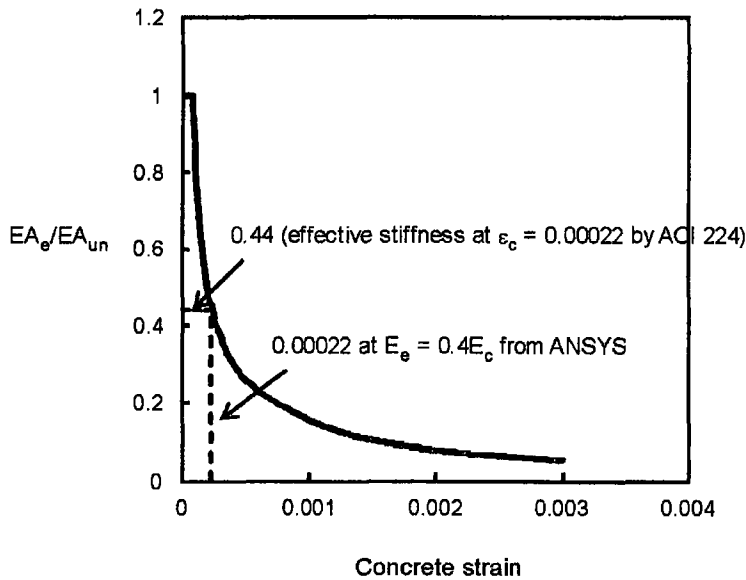


Fig. 1 Relationship between concrete strain and effective stiffness: Vertical direction

2. Hoop direction

ANSYS hoop strain, $\epsilon_{h,ansys}$, of (D+F+1.5P) at restored area: $E_e = 0.4E_c$

$$\epsilon_{h,ansys} := 0.00033$$

Hoop tensile strains corresponding to $E_e = 0.4E_c$ from ANSYS

Calculation of cracking load

$$A_s := 10.22 \frac{\text{in}^2}{\text{ft}}$$

$$\rho := \frac{A_s}{A_g} = 0.0164$$

$$P_{cr} := (1 - \rho + n \cdot \rho) \cdot A_g \cdot f_t = 211 \cdot \frac{\text{kip}}{\text{ft}} \quad \text{Eq (2.1) of ACI 224}$$

ACI 224 Calculations to find EA_e corresponding to the concrete strain of $\epsilon_{h,ansys}$

Assume an axial load $P := 250 \frac{\text{kip}}{\text{ft}} > P_{cr} = 211 \frac{\text{kip}}{\text{ft}}$ Cracked section

$$A_{cr} := n \cdot A_s \quad \text{Definition given in ACI 224}$$

$$A_e := A_g \cdot \left(\frac{P_{cr}}{P} \right)^3 + A_{cr} \cdot \left[1 - \left(\frac{P_{cr}}{P} \right)^3 \right] = 402 \cdot \frac{\text{in}^2}{\text{ft}} \quad \text{Eq (4.13) of ACI 224}$$

$$EA_e := E_c \cdot A_e = 1773981 \cdot \frac{\text{kip}}{\text{ft}}$$

$$\frac{EA_e}{EA_{un}} = 0.644 \quad E_{cr} := \frac{EA_e}{EA_{un}} \cdot E_c$$

$$\epsilon_v := \frac{P}{EA_e} = 0.00014$$

By repeating the calculation for different axial loads, P, the relationship between the concrete strain and the corresponding effective stiffness can be obtained. The following figure shows the resulting relationship.

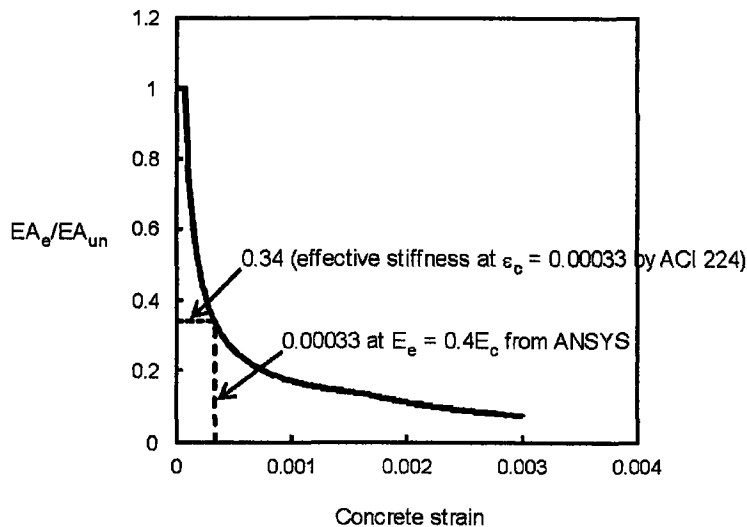


Fig. 2 Relationship between concrete strain and effective stiffness: Hoop direction

From Figures 1 and 2, the ratio of effective stiffness in ACI 224.2R to that of ANSYS can be calculated as follows:

$$\text{Vertical direction: } (E_c)_{ACI224}/(E_c)_{ANSYS} = 0.44/0.40 = 1.10$$

$$\text{Hoop direction: } (E_c)_{ACI224}/(E_c)_{ANSYS} = 0.34/0.40 = 0.85$$

$$\text{Average difference in both direction: } (1.10+0.85)/2 = 0.98$$

These points are reported in Figure H.2 of Calculation C-257-01.04.06 (Ref. 2).

RAI 4

From Section 8.1.2.2, "Cracked Conditions," and Appendix H of Calculation C-257-01.04.06 (Reference 2), it appears that the same value of reduced concrete section stiffness ($A_e E_c$) of $0.4E_c A_g$ was used in the model for each of the load combinations III, IV, and VI.

Please confirm if this is true. If so, please provide the justification for using the same value for all the load combinations, considering the fact that the axial strains and the extent of concrete cracking, and therefore the sectional stiffness, is a function of the magnitude of the forces due to the applied loads.

Response to RAI 4

A single value of $0.4E_c A_g$ was used in the model for load combinations III, IV and VI. The reduced section stiffness of $0.4E_c A_g$ was derived based on load combination III (D+F+1.5P), for which the most severe cracking condition is expected as explained below.

The containment structure is under bi-axial compression under operating conditions and therefore, full stiffness is expected throughout containment wall and dome due to continuity of the prestressing system. Since the construction opening is away from any discontinuities, the membrane forces will be the dominant factor in the behavior of the wall in this area. In case of a LOCA accident, internal pressure decreases the membrane compression in the structure. The maximum decrease in membrane compression will occur under the loading combination that includes 1.5P. Since the prestressing tendons are continuous, the membrane forces are expected to remain constant throughout the wall and dome. However, it is conceivable that membrane compression may be reduced in the construction opening area, resulting in membrane tension, thus leading to small cracks. This in turn may lead to re-distribution of the internal forces. For this reason, the analysis was performed to determine the maximum possible reduction in stiffness and the consequent re-distribution of internal forces.

The phenomenon described above is best understood from a review of the figures in Appendix G of Ref. 2 which illustrate the state of stress in the repair and surrounding areas as the work progresses. Figure G.1 shows the construction sequence, from (a) to (f), Figures G.2 and G.3 show the corresponding state of stress in the vertical and horizontal directions, respectively (these figures are not to scale, i.e., the

forces shown are qualitative only; however, these figures are based on ANSYS analyses). The following may be observed from a review of Figure G.2:

- Fig. G.2 (b) shows that membrane compression in the vertical direction is zero under dead load once the opening is cut (Fig. G.1, stages (c) through (f)). Membrane compression due to dead load is never restored in the repair area.
- Fig. G.2 (c) shows that vertical membrane force is reduced when partial tendon de-tensioning is achieved (Fig. G.1 (b)), and it is zero when the opening is cut (Fig. G.1 (c)).
- Fig. G.2 (d) shows that as creep and shrinkage take place, membrane compression is reduced in the repair area and increased in the adjacent areas (i.e., transfer of membrane forces).
- Fig. G.2 (e) shows the final state of stress in the area corresponding to Fig. G.1 (e). As shown in this figure, the membrane compression in the repair area is significantly less than the adjacent wall segments due to the reduced stiffness. If the stiffness in the repair area were assumed to be zero, the membrane compression would be zero.
- Fig. G.2 (e) indicates that membrane compression adjacent to the repair area is higher than it was before the opening was made. Also, it shows that, after the completion of the prestressing of the replacement tendons, the membrane compression will not reach to the level of the undisturbed containment wall. If the internal pressure is applied in the condition of Fig. G.2 (e), it is easy to visualize that the membrane compression in the opening area will become tension and therefore, it is prudent to consider the possibility of cracking in this area.

As the above summary of the analysis procedure implies, one goal of the analysis methodology was to determine maximum possible increase in the membrane forces and moments in areas surrounding the opening so that adequacy of the existing design can be demonstrated. Since load combination III generates the maximum membrane tension due to internal pressure, it is expected to provide an upper-bound design condition in the surrounding area, in conjunction with a large decrease in axial stiffness (from 1.0 down to 0.4). Therefore, the calculation of the reduced stiffness based on the load combination III is adequate.

RAI 5

The methodology used in the parametric study in Appendix H of Calculation C-257-01.04.06 (page 84 of Reference 2) and the ANSYS containment analyses accounting for cracking is based on the assumption that the reduced effective axial stiffness ($A_e E_c$) for the hoop and vertical directions are equal. Please justify this assumption considering the fact that the degree of cracking is likely to not be the same in the two directions.

Response to RAI 5

The SONGS UFSAR description of the method of evaluation for the containment structure is contained in UFSAR 3.8.1.4 (Ref. 14) with detailed instructions contained in BC-TOP-5, Rev. 1 (Ref. 5). The analysis “consists of two parts, the overall analysis ... and the local analysis.” The overall analysis employs an axisymmetric model of the containment structure that takes advantage of the basic radial symmetry of the structure about the vertical axis to reduce the model size. The overall analysis, however, does not account for non-symmetric features such as buttresses, penetrations, brackets, and liner plate anchors. These features are considered in the local analysis, which employs a variety of evaluation techniques, depending on the specific feature, including testing (for tendon anchorages), computer programs (for large penetration openings, such as the equipment hatch), and manual calculation methods (for small penetration openings and anchors).

The temporary SGR opening meets the UFSAR definition of a large penetration: “having an inside diameter equal to or greater than 2.5 times the nominal shell thickness.” Even though the concrete and tendons are ultimately restored, the temporary SGR opening introduces a permanent, non-symmetric redistribution of prestress loads similar to, although not as pronounced as, a large penetration opening. Calculation C-257-01.04.06 (Ref. 2) was performed to account for the permanent effects of the restored temporary SGR opening. This re-analysis of the containment was performed using the methods for evaluating large penetration openings contained in UFSAR 3.8.1.4 and BC-TOP-5, Rev. 1.

Calculation C-257-01.04.06 (Ref. 2) does not supersede the overall analysis or various local analyses of the original containment analysis. Instead, this calculation provides a supplemental local analysis that accounts for redistribution of stresses in the areas within and surrounding the restored temporary SGR opening. The goal of this calculation was to evaluate the restored temporary SGR opening following the UFSAR-described methods of evaluation and applying the same structural acceptance criteria used in the original containment design. In that case, it would not have been appropriate to apply methods and acceptance criteria different from SONGS original containment design.

The analysis was done by considering a severe condition in an approximate, yet conservative manner. The restored area will find the equilibrium conditions since the more it cracks, the more the forces will be redistributed to the surrounding area. As such, the critical area for checking the structural integrity of the containment is the surrounding area of the temporary opening. The analysis approach taken in Calculation C-257-01.04.06 (Ref. 2) was to use a reduced stiffness value which will provide

reasonable upper-bound estimate for both hoop and vertical directions while providing conservative results.

It is also important to note that this concept of reducing the concrete stiffness for both hoop and vertical directions simultaneously by reducing concrete modulus of elasticity is consistent with methodology provided in Section 7.2.1.2 and 7.2.1.4 of BC-TOP-5, Rev.1 (Ref. 5).

RAI 6

- (a) The ANSYS parametric analyses in Appendix H of Reference 2 used the same effective axial stiffness $[(E_oA_e)_{ANSYS}]$ values for the hoop and vertical directions (see assumption described in RAI 5). However, the criterion used in Appendix H (page 84 of Reference 2) to determine the convergence of the effective sectional stiffness values between the parametric ANSYS analyses and the ACI 224.2R-estimated values [for the two directions] does not seek to satisfy nor does it satisfy the assumption that the effective stiffness in the two directions are considered equal. Instead, it averages the ACI 224.2R-estimated vertical and horizontal effective stiffness (see Figure H.2 in Appendix H of Reference 2). The average curve so obtained intersects the line representing the ratio $(E_oA_e)_{ACI224}/(E_oA_e)_{ANSYS} = 1$ at two points corresponding to the ratio, $(E_oA_e)_{ANSYS}/E_oA_g$, of 0.4 and 0.7. It can be noted from Figure H.2 that the ACI 224.2R-estimated effective stiffness are not equal in the two directions for both of these values. The smaller of the two values (with no explanation provided), $0.4E_oA_g$, was selected as the reduced effective stiffness and was used for the containment opening area in the concrete cracking analysis, even though the larger value would occur earlier when cracking occurs.

Please explain the basis for the criterion used to determine the effective stiffness value with regard to the SONGS containment analysis.

Response to RAI 6(a)

Calculation C-257-01.04.06 (Ref. 2) provides a supplemental local analysis that accounts for redistribution of stresses in the areas within and surrounding the restored temporary SGR opening. The critical area for the structural integrity is the surrounding area. As such, the use of smaller reduced stiffness provides the more conservative estimate for design requirements.

- (b) Assuming that the data and assumptions in Figure H.2 are correct, it appears that the appropriate criterion to be used to determine the converged value of the effective axial stiffness between the ANSYS parametric study and the ACI 224.2R-estimated values should be the value of $(E_c A_e)_{ANSYS}$ for which:

$$[(E_c A_e)_{ACI224}/(E_c A_e)_{ANSYS}]_{Hoop} = [(E_c A_e)_{ACI224}/(E_c A_e)_{ANSYS}]_{vertical} = \sim 1$$

This criterion also satisfies the assumption that the effective stiffness in the two directions are equal. These ratios for the two directions are not expected to converge exactly to 1 because of the approximations in the 1-dimensional ACI 224.2R method relative to the 3-dimensional ANSYS parametric analyses, but would likely be roughly close to 1.

Accordingly, from Figure H.2 on page 84 of Reference 2, the converged value of the reduced effective axial stiffness to be used in the SONGS containment analysis would be the value corresponding to the intersection of the vertical and hoop curves, which is $0.55E_c A_g$, with the ratio $(E_c A_e)_{ACI224}/(E_c A_e)_{ANSYS}$ being approximately 0.9 (close to 1).

Regarding this approach, please address the impact of the noted difference in the effective stiffness value on the SONGS end-of-life containment analyses, while also considering the questions raised in all of the other RAIs. Alternatively, please justify why the value of effective stiffness used ($0.4E_c A_g$) by the licensee is appropriate, considering the issues raised in paragraph (a) above and in all of the other RAIs, as applicable.

Response to RAI 6(b)

Please refer to the responses given for RAI 4 and 5. The correct value of effective stiffness may vary depending on the directions and the load combination used. As stated in response to previous questions, the critical design goal here is to maximize the redistribution of the forces to the surrounding area to assure design adequacy in case the stiffness is reduced in the repair area. The greater the reduction in effective stiffness value, the greater the re-distribution. The effective stiffness factor of 0.4 is a reasonable lower-bound value. Further reduction in stiffness would lead to unrealistic design requirements. A higher value of the reduced stiffness would result in lower forces in the surrounding area. Therefore, the use of the lowest possible effective stiffness ($0.4E_c A_g$) will maximize the redistribution of the forces to the surrounding area to assure design adequacy.

RAI 7

Assuming that the forces and moments at the concrete sections expected to be cracked, obtained on the basis of the uncracked ANSYS analysis, are reacted entirely by the combination of unbonded prestressing tendons and bonded reinforcing steel, please provide the following information for each of the hoop and vertical directions for the critical load combinations in the SONGS containment EOL analysis:

- (a) the maximum tensile stress in the prestressing tendons,
- (b) the maximum tensile stress in the reinforcement for the primary forces in the load combination,
- (c) the maximum tensile stress and the maximum strain in the bonded reinforcement for the combined primary and secondary forces in the load combination, and
- (d) the maximum stress and strain, as appropriate, in the liner (please indicate if tensile or compressive).

Response to RAI 7

The following table shows the requested information for each direction:

	Vertical direction	Hoop direction
(a) maximum tensile stress in the prestressing tendons	183 ksi	177 ksi
(b) maximum tensile stress in the reinforcement for the primary forces	47 ksi	52 ksi
(c) maximum tensile stress and the maximum strain in the bonded reinforcement for the combined primary and secondary forces	51 ksi (1745×10^{-6} in./in.)	48 ksi (1655×10^{-6} in./in.)
(d) maximum stress and strain in the liner	-22 ksi (-775×10^{-6} in./in.)	24 ksi (= $f_{y,liner}$) (2207×10^{-6} in./in.)

Note: (+) Tension
(-) Compression
 $f_{y,liner}$ = Yield strength of the liner

RAI 8

Concrete cracking could also result in reduction in flexural stiffness and shear stiffness that could contribute to redistribution of moments and forces, which have not been considered in the SONGS analyses accounting for concrete cracking in Reference 2. Therefore, please provide

the justification as to why the end-of-life evaluation of the SONGS containment following steam generator replacement in Reference 2 selectively considered only reduction in axial tensile stiffness, and resulting redistribution of tensile membrane forces, due to concrete cracking.

Response to RAI 8

The stiffness study described in Ref. 2 and the resulting “effective stiffness” was based on axial behavior of a one-dimensional concrete element. The effective stiffness was modeled simply using a reduced modulus of elasticity.

Using this method, the axial stiffness will be proportional to:

$$R_{\text{axial}} \propto E_r \times A$$

and bending and shear stiffnesses will also be proportional to:

$$R_{\text{bending}} \propto E_r \times I$$

$$R_{\text{shear}} \propto E_r / 2(1+\nu) \times A$$

where E_r is the effective modulus, A is the section area and ν is the Poisson’s ratio. Thus, the flexural stiffness and shear stiffness are reduced by the same “effective modulus” ratio. The analyses results obtained by using the 0.4 effective stiffness values were included in Ref. 2. In the following, the effects of reduced stiffness in the repair area will be examined for both flexure and shear.

Flexure

As shown in Figures 9 and 10 of Ref. 2, the bending moments in both horizontal and vertical directions are reduced compared with the original design values. As expected, the bending moments in the surrounding areas are increased, as shown in Figures 11 and 11A. Tables 12 and 12A indicate the same trend in terms of element stresses. Therefore, the goal of maximizing the axial forces and bending moments in the surrounding area is realized.

It is recognized that the reduction in bending stiffness may be greater than implied by the above approximation. However, the primary parameter affecting the repair area behavior is the axial force and not the bending moment. Therefore, the potential uncertainty introduced by the above approximation is insignificant. It is also important to note that the conservative approximations made in the analyses to maximize the cracking predicted by the analysis in the opening area. Review of Figures 9 and 10 in Ref. 2 indicates that the resulting design forces under all load combinations are entirely within the allowable interaction diagram. Similarly, review of Tables 12 and 12A in Ref. 2 shows that the maximum stresses, which represent the stresses at a point in the most critical element (without any averaging), are far less than the allowable values.

Therefore, the simplified stiffness modeling used in the repair area analysis is adequate and conservative.

The adequacy of the repair area was further justified by the results of the crack mapping programs for both Units 2 and 3 after the repairs, during the Integrated Leak Rate Test (ILRT). The results of the crack mapping are included in Ref. 9 through Ref. 12. Review of the ILRT test data lead to the following conclusions:

- In all cases, the maximum measured crack width in the repair area was less than 0.013” or 0.33 mm,

- Any cracks that appeared when the structure was under the ILRT pressure were less than 0.2 mm,
- Cracks that appeared during the pressurization closed upon completion of the test,
- Nothing unusual or significant was observed during these tests.

The above observations confirm the statements that the containment analyses for SONGS SGR were performed with assumptions that resulted in a conservative design in the repair area.

Shear

In the case of shear, the in-plane and out-of-plane results should be considered separately:

- **Tangential (In-Plane) Shear:**

Since the containment is an axisymmetric structure and the repair area is away from any discontinuities, the only source of significant in-plane shear is the earthquake load. This is the “tangential shear” and has been evaluated in Section 8.1.2.3 of Ref. 2. The maximum design forces as calculated in that reference are summarized below:

Direction	Load Combination	Reinforcement Demand, in ² /ft	Reinforcement Provided, in ² /ft	Demand/Capacity Ratio
Vertical	IV	3.9	5.2	0.75
Hoop	VI	2.6	4.8	0.54

If it is assumed that the wall in the repair area is ineffective in resisting any tangential shear, the demand capacity ratio in the remainder of the wall can be approximated by:

$$(A_s)_{\text{demand}} = L/(L - L_o) = (\pi \times 77\text{ft}) / (\pi \times 77\text{ft} - 32\text{ft}) = 1.15$$

where L is the one-half containment perimeter and L_o is the width of the opening area.

Thus, the demand in the remaining segment of the wall would be increased by about 15%.

$$D/C = 0.75 \times 1.15 = 0.86$$

The above simple check shows that the containment wall has sufficient capacity to resist the tangential shear that may be imposed on it by the design basis earthquake.

- **Out-of-Plane Shear:**

In the case of the out-of-plane shear, the shear stresses are very small in the repair and surrounding areas due to continuity of the containment structure. Stiffness reduction in the repair area will have negligible effects on out-of-plane shear stresses in the restored and surrounding areas.

In addition, radial ties (#8 @ 1°) were provided in the repair area, following the original rebar drawing of the containment wall. As such, radial ties are placed at repair and surrounding areas to resist any radial tension.

References:

1. Calculation No. C-257-01.04.05, ECP No. 061200409-6, R0, Evaluation of Restored Containment - Concrete Modulus Ratio and Tendon Retensioning Forces, SONGS, Unit 2 and Unit 3.
2. Calculation No. C-257-01.04.06, ECN/Prelim CCN No. D0020134, Evaluation of Restored Containment End-of-Life Analysis, SONGS, Unit 2 and Unit 3.
3. UCB/SESM-1979/05, "Studies of Concrete for San Onofre Nuclear Power Plant Containment Structures, Units 2 & 3," Structural Engineering Laboratory, University of California, Berkeley, California, 54 pp.
4. ASTM C 512-02, "Standard Test Method for Creep of Concrete in Compression."
5. BC-TOP-5, Revision 1, "Prestressed Concrete Nuclear Reactor Containment Structures," Dec. 1972.
6. ACI 209R-92, "Prediction of Creep, Shrinkage, and Temperature Effects in Concrete Structures."
7. ACI 224.2R-92, "Cracking of Concrete Members in Direct Tension."
8. CTL Group, 25221-000-HC4-SY01-0002, "Final Report for ASTM C 512 Creep and Shrinkage, San Onofre Nuclear Generating Station Units 2 and 3, Steam Generator Replacement Project," 5 pp.
9. Inspection Report SO23-XXIV-3.8.3, Rev.0, "In Process Visual Examination of the Temporary Containment Opening – SONGS Unit 2," 14 pp.
10. Examination Report SO23-XXIV-3.8.1, "Visual Examination of the Containment Construction Opening Concrete Surface prior to ILRT – SONGS Unit 3," 16 pp.
11. Examination Report SO23-XXIV-3.8.1, "Visual Examination of the Containment Construction Opening Concrete Surface at ILRT Test Pressure– SONGS Unit 3," 8 pp.
12. Examination Report SO23-XXIV-3.8.1, "Visual Examination of the Containment Construction Opening Concrete Surface After the ILRT – SONGS Unit 3," 6 pp.
13. Collins, M.P. and Mitchell, D., "Prestressed Concrete Structures," Response Publications, Canada, 1997, 766 pp.
14. San Onofre Units 2 and 3 Updated Final Safety Analysis Report (UFSAR), Rev.22.

Attachment(s):

1. Summary Sheets of Tendon Retensioning Activity for Units 2 and 3, 2 pp.

UNIT 2

1. Date for concrete pouring:

12/19/2009 (Ref. doc : 1)

2. Tendon retensioning

Vertical Tendon

ID	Date
48 - 104	NA
49 - 103	NA
50 - 102	12/31/2009
59 - 3	1/3/2010
60 - 2	1/3/2010
61 - 1	1/3/2010
62 - 180	1/1/2010
63 - 179	1/1/2010
64 - 178	1/1/2010
65 - 177	1/4/2010
66 - 176	1/4/2010
67 - 175	1/4/2010
68 - 174	1/1/2010
69 - 173	1/1/2010
70 - 172	1/2/2010
71 - 171	1/4/2010
72 - 170	1/4/2010
73 - 169	1/4/2010
74 - 168	1/2/2010
75 - 167	1/2/2010
76 - 166	1/2/2010
77 - 165	1/4/2010
78 - 164	1/4/2010
79 - 163	1/4/2010
80 - 162	1/1/2010
81 - 161	1/1/2010
82 - 160	1/1/2010
83 - 159	1/3/2010
84 - 158	1/3/2010
85 - 157	1/3/2010
86 - 156	12/31/2009
87 - 155	12/31/2009
88 - 154	12/31/2009
99 - 53	1/2/2010
100 - 52	1/2/2010
101 - 51	1/2/2010
Ref. doc	2

Hoop Tendon Group 1

ID	Date
14	1/2/2010
17	1/2/2010
20	1/2/2010
23	1/4/2010
26	1/3/2010
29	1/3/2010
32	1/3/2010
35	1/3/2010
38	1/3/2010
41	1/3/2010
44	1/3/2010
47	1/2/2010
50	1/2/2010
53	1/1/2010
56	1/1/2010
59	1/1/2010
62	1/1/2010
65	1/1/2010
68	1/1/2010
71	1/1/2010
74	12/31/2009
77	12/31/2009
80	12/31/2009
Ref. doc	3

Hoop Tendon Group 2

ID	Date
15	12/31/2009
18	12/31/2009
21	12/31/2009
24	12/31/2009
27	1/2/2010
30	1/1/2010
33	1/1/2010
36	1/1/2010
39	1/2/2010
42	1/2/2010
45	1/2/2010
48	1/4/2010
51	1/4/2010
54	1/4/2010
57	1/3/2010
60	1/3/2010
63	1/3/2010
66	1/3/2010
69	1/3/2010
72	1/3/2010
75	1/3/2010
78	1/3/2010
81	1/2/2010
Ref. doc	4

References:

1. Turnover Package No. 25221-002-COT-3054-00127 Dated 4/9/10,
Construction Opening Formwork and Concrete Placement
2. Turnover Package No. 25221-002-COT-3051-00119 Dated 2/8/10,
Vertical Tendon Removal and Installation
3. Turnover Package No. 25221-002-COT-3051-00121 Dated 1/21/10, Unit 2
Removal/Reinstallation of Horizontal Tendons Buttress 1A & 3B
4. Turnover Package No. 25221-002-COT-3051-00123 Dated 2/9/10,
Removal/Reinstallation of Horizontal Tendons between Buttress 3A & 2B for Unit 2

UNIT 3

1. Date for concrete pouring:

12/16/2010 (Ref. doc : 1)

2. Tendon retensioning

Vertical Tendon

ID	Date
48 - 104	12/22/2010
49 - 103	12/23/2010
50 - 102	12/23/2010
59 - 3	12/26/2010
60 - 2	12/26/2010
61 - 1	12/26/2010
62 - 180	12/24/2010
63 - 179	12/24/2010
64 - 178	12/24/2010
65 - 177	12/27/2010
66 - 176	12/27/2010
67 - 175	12/27/2010
68 - 174	12/26/2010
69 - 173	12/26/2010
70 - 172	12/26/2010
71 - 171	12/28/2010
72 - 170	12/28/2010
73 - 169	12/28/2010
74 - 168	12/26/2010
75 - 167	12/26/2010
76 - 166	12/26/2010
77 - 165	12/27/2010
78 - 164	12/27/2010
79 - 163	12/27/2010
80 - 162	12/25/2010
81 - 161	12/25/2010
82 - 160	12/24/2010
83 - 159	12/27/2010
84 - 158	12/27/2010
85 - 157	12/26/2010
86 - 156	12/23/2010
87 - 155	12/23/2010
88 - 154	12/23/2010
99 - 53	12/25/2010
100 - 52	12/25/2010
101 - 51	12/25/2010
Ref. doc	2

Hoop Tendon Group 1

ID	Date
14	12/25/2010
17	12/25/2010
20	12/25/2010
23	12/25/2010
26	12/26/2010
29	12/26/2010
32	12/26/2010
35	12/26/2010
38	12/27/2010
41	12/28/2010
44	12/28/2010
47	12/28/2010
50	12/27/2010
63	12/27/2010
56	12/27/2010
59	12/27/2010
62	12/27/2010
65	12/27/2010
68	12/24/2010
71	12/23/2010
74	12/23/2010
77	12/23/2010
80	12/23/2010
Ref. doc	3

Hoop Tendon Group 2

ID	Date
15	12/23/2010
18	12/23/2010
21	12/23/2010
24	12/23/2010
27	12/24/2010
30	12/27/2010
33	12/27/2010
36	12/27/2010
39	12/27/2010
42	12/28/2010
45	12/28/2010
48	12/28/2010
51	12/28/2010
54	12/27/2010
57	12/26/2010
60	12/26/2010
63	12/26/2010
66	12/26/2010
69	12/25/2010
72	12/25/2010
75	12/25/2010
78	12/25/2010
81	12/25/2010
Ref. doc	4

References:

1. Turnover Package No. 25221-003-COT-3054-00127 Dated 2/9/11,
Containment Constuction Opening - Formwork and Concrete Placement
2. Turnover Package No. 25221-003-COT-3051-00119 Dated 1/24/11,
Remove and Replace Vertical Tendons for Unit 3 SGR
3. Turnover Package No. 25221-003-COT-3051-00121 Dated 1/25/11,
Remov/Replace and degrease Horizontal Tendons Between Buttress 1A-3B
4. Turnover Package No. 25221-003-COT-3051-00123 Dated 1/25/11,
Remov/Replace and degrease Horizontal Tendons Between Buttress 2B-3A